



ORIGINAL ARTICLE

Novel silver-platinum bimetallic nanoalloy synthesized from *Vernonia mespilifolia* extract: Antioxidant, antimicrobial, and cytotoxic activities



Jeremiah O. Unuofin^a, Adewale O. Oladipo^{b,*}, Titus A.M. Msagati^b,
Sogolo L. Lebelo^a, Stephen Meddows-Taylor^c, Garland K. More^c

^a Department of Life and Consumer Sciences, College of Agriculture and Environmental Sciences, University of South Africa, Science Campus, Florida, Johannesburg 1710, South Africa

^b Nanotechnology and Water Sustainability Research Unit, College of Science, Engineering and Technology, University of South Africa, Science Campus, Florida, Johannesburg 1710, South Africa

^c College of Agriculture and Environmental Sciences Laboratories, University of South Africa, Science Campus, Florida, Johannesburg 1710, South Africa

Received 18 April 2020; accepted 16 June 2020

Available online 25 June 2020

KEYWORDS

Antibacterial;
Antioxidant;
Bimetallic nanoparticles;
Cytotoxicity;
Vernonia mespilifolia

Abstract In this study, bimetallic nanoparticles comprising silver and platinum with promising therapeutic activities were synthesized using ethanolic *Vernonia mespilifolia* plant extract for the first time. The bimetallic silver-platinum nanoparticles (AgPtNPs) were characterized using solid-state techniques including UV–vis spectroscopy, Fourier transform infrared spectroscopy (FTIR), transmission electron microscopy (TEM), and energy-dispersive X-ray spectroscopy (EDX) techniques. The internal morphological structure showed that the AgPtNPs were spherical with a diameter of approximately 35.5 ± 0.8 nm, while FTIR confirmed the effective capping and formation of the nanoparticles by phytoconstituents. The polyphenolic contents of the green synthesized nanoparticles from the ethanolic extract of *V. mespilifolia* (AgNPs and AgPtNPs) was found to be $(28.0 \pm 0.8$ and 13.6 ± 0.1 mg GAE/g) total phenol, while the flavonoids content was $(366.2 \pm 17.0$ and 126.6 ± 0.2 mg QE/g), and proanthocyanins content was $(161.8 \pm 0.6$ and 70.2 ± 0.6 mg CE/g). The AgPtNPs displayed a greater ability to scavenge free radicals, especially DPPH and ABTS (IC₅₀ 19.5 and 21.6 μg/mL) respectively when compared with AgNPs and ascorbic acid. Besides, the AgPtNPs had a higher ferric reducing antioxidant power (FRAP) (44.1 mg GAE/g) when compared to AgNPs (18.5 mg GAE/g). Moreover, the AgPtNPs showed a two-fold antimicrobial activity towards pathogenic microbes compared to AgNPs and a selective

* Corresponding author.

E-mail address: walex20002001@gmail.com (A.O. Oladipo).

Peer review under responsibility of King Saud University.



Production and hosting by Elsevier

cytotoxic potency towards MCF-7 breast cancer cell line compared to HEK 293 normal cell line. In summary, these fascinating bioactivities displayed by the AgPtNPs highlighted their potential in therapeutic biomedical applications.

© 2020 The Authors. Published by Elsevier B.V. on behalf of King Saud University. This is an open access article under the CC BY-NC-ND license (<http://creativecommons.org/licenses/by-nc-nd/4.0/>).

1. Introduction

The deployment of noble metal nanoparticles in many multi-disciplinary fields such as biomedical applications have improved the general treatment outcomes against many degenerative diseases like cancer and Alzheimer's. Nanoparticles of noble metal sources have recently attracted the attention of many researchers recently, due to their unique optical and electronic properties, unlike their bulk counterparts (Fakayode et al., 2016; Oladipo et al., 2017). Diverse approaches to nanoparticles synthesis like physical, and chemical methods have been well established (Nath and Banerjee, 2013; Srinoi et al., 2018). However, concerns over the use of toxic and hazardous chemicals for their synthesis and stabilization have limited their medical applications (John Leo and Oluwafemi, 2017; Mohan et al., 2014). Consequently, the demand for an eco-friendly route for the synthesis of nanoparticles beneficial to human health has received extensive consideration. The use of green and biogenic synthetic methodologies in the last decade using plants and microbes has become preferable and are being widely investigated. Many outstanding reviews on the use of biologically abundant materials such as plant extracts, bacteria, fungi, and metabolites have provided a benign method of synthesis of nanoparticles with significant biological activities.

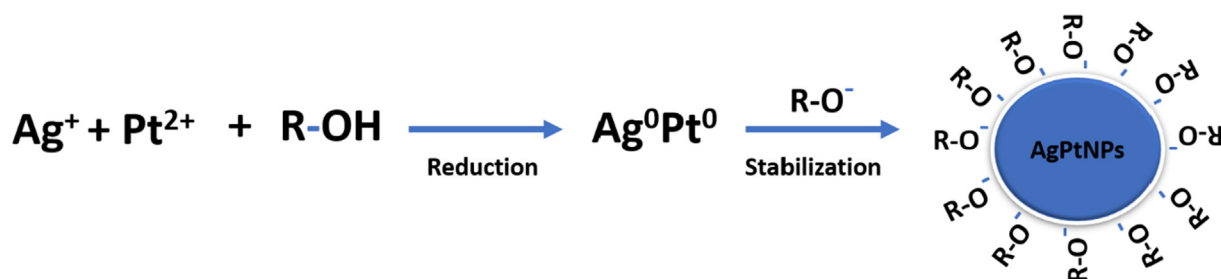
In the last few decades, bimetallic nanoparticles have become more attractive in biomedical fields as well as in catalytic, optical, and electronic applications compared to monometallic nanoparticles. This trend has been attributed to their synergistic ability to combine the properties of two individual metals in a single entity (Meena Kumari et al., 2015; Oladipo et al., 2020b; Sharma et al., 2019). Many bimetallic combinations such as those of silver-gold (Adebayo et al., 2019; Elegbede et al., 2019), gold-platinum (Oladipo et al., 2020a), gold-palladium (Ding et al., 2010), palladium-platinum (Ghosh et al., 2015), platinum-copper (Olajire et al., 2017), and nickel-copper (Seethapathy et al., 2019) with potential antioxidant, anticoagulant and thrombolytic activities have been reported to generate enhanced activities over their individual constituents. In particular, nanoparticles of silver-platinum (AgPt) occurring as bimetallic have attracted scientific interest, mainly due to the peritectic system formed by silver and platinum. Both silver and platinum are two important noble metals with fascinating properties. However, combining this two metal system is generally associated with a broad miscibility gap (Grasmik et al., 2018; Pan et al., 2016).

Since the emergence of multidrug resistance (MDR) problem as a challenge facing many fraternities in clinical and medical practices, the achievements recorded over time in the therapeutic advances have somehow been limited. As a result, there is an urgent need to develop a new, ingenious, and combinatory approach to overcome this trend. In recent years, the

antioxidant (Reddy et al., 2014), and antimicrobial potency (Ojha et al., 2013) of silver nanoparticles as well as the cytotoxic (Baskaran et al., 2017), and reactive oxygen species (ROS) scavenging (Manikandan et al., 2013) properties of platinum nanoparticles have been well reported. While many reports exist on the chemical-mediated synthesis of bimetallic silver-platinum nanoparticles (AgPtNPs), the majority of these nanoparticles' atomic arrangements are core-shell in architecture. For example, Zhang et al fabricated a novel Pt/Ag bimetallic nanoparticle decorated onto a porous reduced graphene oxide (rGO) via a chemical reduction/galvanic replacement process. The hybrid nanocomposite demonstrated enhanced antimicrobial activity against *Escherichia coli* pathogen (Zhang et al., 2016). Breisch et al. synthesized AgPt nanoparticles via a sodium borohydride assisted co-reduction method for combined osteo-promotive and antimicrobial activity (Breisch et al., 2019). Furthermore, an improved anti-cancer and antimicrobial activity of core-shell dendritic-like AgPt nanoparticles was reported (Ruiz et al., 2020). With core-shell bimetallic nanoparticles adjudged to have a high surface area and multiple surfaces (Sharma et al., 2019; Zhang et al., 2017), the activities of homogenous atomic distribution of alloyed bimetallic architecture are yet to be fully elucidated. This has motivated the need to explore the biological response of a bimetallic alloyed system composed of silver and platinum via an environmentally friendly method.

Vernonia mespilifolia is an important shrub widely distributed all over Southern Africa (Robinson and Funk, 2014). Several medicinal potentials such as the treatment of heart disease in ruminant animals and the management of hypertension and body weight have been ascribed to various parts of this plant (Afolayan and Mbaebie, 2010; Dold and Cocks, 2001). Various biological activities such as antiobesity (Unuofin et al., 2019), antioxidant (Unuofin et al., 2018), antimicrobial (Unuofin et al., 2017), antimycobacterial (McGaw et al., 2008), and antitrypanosomal activities (Mokoka et al., 2013) have been attributed to both organic and inorganic solvent extracts of *V. mespilifolia*. These bioconstituents include flavonoids, terpenoids, phenols, etc. are essential bioactive agents capable of mediating nanoparticles synthesis since they can easily bind onto the surfaces thereby stabilize nanoparticles through electrostatic stabilization (Oladipo et al., 2020a). To the best of our knowledge, no report currently exists on the biosynthesis of bimetallic silver-platinum nanoparticles (AgPtNPs) utilizing a whole plant extract of *V. mespilifolia*.

Therefore, as a contribution to the growing interest in nanomedicine, we have explored the possibility of the reducing and capping potentials of whole plant extract solution of *V. mespilifolia* in forming bimetallic alloyed nanoparticles (Scheme 1). The synthesized AgPtNPs presented a hydrophilic stabilized nanohybrid, which was further examined for their potential biological effects, including antioxidant,



Scheme 1 Illustration showing the proposed mechanism of action of the phytochemicals on the formation of AgPtNPs.

antimicrobial, and cytotoxic activities, in comparison to monometallic AgNPs.

2. Experimental

2.1. Materials

Silver nitrate ($AgNO_3$, $\geq 99\%$), potassium tetrachloroplatinate (II) ($K_2PtCl_4 \geq 99.9\%$), Folin-Ciocalteu reagent, anhydrous sodium carbonate, aluminum trichloride ($AlCl_3$), sodium nitrite ($NaNO_2$), sodium chloride ($NaCl$), 2,2-diphenyl-1-picrylhydrazyl (DPPH), 2,2'-azino-bis (3-ethylbenzothiazoline-6-sulfonic acid) (ABTS), vanillin, TPTZ (tripyrindyl triazine), Mueller Hinton agar, Mueller Hinton broth, 3-(4,5-dimethylthiazol-2-yl)-2,5-diphenyltetrazolium bromide (MTT), Dulbecco's Modified Eagle's Medium (DMEM) supplemented with 10% fetal bovine serum (FBS), 1% penicillin-streptomycin solution, sodium acetate, ferric chloride, ascorbic acid, hydrochloric acid, sodium hydroxide, and phosphate buffer. All chemicals used in this study were of analytical grade and purchased from Sigma-Aldrich (Johannesburg, South Africa). Whole *V. mespilifolia* plants were collected and identified by Mr. Tony Dold of Selmar Schonland Herbarium, Rhodes University, South Africa. All solutions were prepared with deionized water.

2.2. Preparation of plant material and extract

V. mespilifolia was prepared as previously reported (Unuofin et al., 2018). 1 g of finely ground powder of *V. mespilifolia* whole plant was mixed with 100 mL ethanol and heated at 60 °C for 20 min and then filtered. The plant extract was kept at 4 °C until further use.

2.3. Synthesis of AgNPs and AgPtNPs and UV-Vis spectroscopy

To synthesize AgPtNPs, 10 mL of ethanolic extract of *V. mespilifolia* (EVM) was mixed with 50 mL of 1 mM $AgNO_3$ and 1 mM of K_2PtCl_4 solution in a flask and stirred at 85 °C for 60 min. The reaction was monitored with UV-vis absorption spectroscopy (PerkinElmer Lambda 60 UV-vis spectrophotometer). The nanoparticles that were obtained were centrifuged and washed several times with water to remove any unreacted salts and extracts. The pellets obtained were then oven-dried at 40 °C to obtain the nanoparticles in powder. As a control, the same procedure was followed to synthesize monometallic AgNPs. The nanoparticles of desired

weight were dispersed in deionized water, sonicated for 10 min and used for further characterization and biological applications unless otherwise stated.

2.4. Characterization

Dried powdered samples of the purified nanoparticles were used for characterization. The FTIR spectra of extract-reduced AgNPs and AgPtNPs were studied using a PerkinElmer Frontier FT-IR fitted with an ATR detector in the range of 4000–500 cm^{-1} . The morphology and particle size of the nanoparticles were determined by dropping a dispersed solution of the purified nanoparticles onto a carbon coated copper grid and then allowed to dry before analysis using transmission electron microscopy (TEM) on a JEOL JEM 2100 running at 200 kV voltage. Energy dispersive X-ray spectra (EDS) were obtained using a TEM equipped with EDS. Nanoparticle stability was determined using Dynamic Light Scattering (DLS) technique on a Malvern Zetasizer Nano-ZS (Malvern Corp, UK).

2.5. Quantitative phytochemical analysis and antioxidant properties

2.5.1. Total phenolic content determination

The quantitative total phenolic content of the synthesized nanomaterial was determined using the Folin-Ciocalteu method, with slight modifications to our previous work (Unuofin et al., 2018). 30 μ L of sample solution (1 mg/mL in water) and standard gallic acid (0.02–0.1 mg/mL) was mixed with 90 μ L Folin-Ciocalteu reagent in 96 well plates and allowed to stand for 5 mins. Then, 120 μ L of 7.5% sodium carbonate was added, and the resultant mixture was incubated at 40 °C for 30 min for color development and then the absorbance was read at 765 nm (Thermo Scientific Varioskan Flash Spectrophotometer, Finland). All experimental set-ups were conducted in triplicates. The total phenolic content (TPC) was calculated in terms of gallic acid equivalent (GAE), in mg/g sample, using a gallic acid calibration curve ($R^2 = 0.98$).

2.5.2. Total flavonoids content determination

The total amount of flavonoids in the synthesized nanomaterial was determined by a modified aluminum chloride method with slight modifications to our previous work (Unuofin et al., 2017). 30 μ L of sample solution (1 mg/mL) or standard catechin at different concentrations (0.2–1 mg/mL) were pipetted into each well. Following this, 192 μ L of distilled H_2O was added, and then 9 μ L of the prepared 5% $NaNO_2$ was added.

After 5 min of rest at room temperature, a further 9 μL of 10% AlCl_3 was added and left to rest for 6 min. 60 μL of 4% NaOH was then added and incubated for 15 min to allow for color development. All measurements were carried out in triplicate. The absorbance was measured at 420 nm (Thermo Scientific Varioskan Flash Spectrophotometer, Finland). The total flavonoid content (TFC) was expressed as QE in mg/g sample ($R^2 = 0.99$).

2.5.3. Proanthocyanidin (Condensed Tannin)

The determination of the proanthocyanidin content of the synthesized nanomaterial was determined according to a method previously described (Hanen et al., 2009). 30 μL of sample solution (1 mg/mL) or standard catechin at different concentrations (0.2–1 mg/mL) were pipetted into each well. This was closely followed by the addition of 180 μL of 4% vanillin-methanol and 90 μL of HCl . This mixture was then vortexed and allowed to stand at room temperature for 15 min. The absorbance was measured at 500 nm (Thermo Scientific Varioskan Flash Spectrophotometer, Finland). Proanthocyanidin content was revealed in terms of catechin equivalent (CE), in mg/g sample, using a catechin calibration curve ($R^2 = 0.99$).

2.6. Quantification of radical scavenging activity

The radical scavenging capacities of AgNPs and AgPtNPs were measured using DPPH radical scavenging activity, ABTS radical scavenging activity, and ferric reducing antioxidant power (FRAP) assay.

2.7. DPPH (2, 2-diphenyl-1-picrylhydrazyl) radical scavenging activity assay

The antioxidant potential of AgNPs and AgPtNPs against DPPH radicals was determined using a previously described method with slight modifications (Khan et al., 2012). The DPPH assays were performed in 96 well plates. The test sample (100 μL) from a stock solution was poured into the respective wells of the plate and then 100 μL of DPPH solution was added to each well to make 200 μL final volume. Ascorbic acid was used as the reference standard. The mixture was incubated at room temperature for 30 min.

$$\text{DPPHscavengingactivity}(\%) = \frac{\text{Abscontrol} - \text{Absample}}{\text{Abscontrol}} \times 100$$

where Abs control is the absorbance of DPPH + methanol and Abs sample is the absorbance of DPPH radical + sample/or standard.

2.8. ABTS (2, 2'-azino-bis (3-ethylbenzothiazoline)-6-sulfonic acid) radical scavenging activity

The ABTS radical scavenging abilities of AgNPs and AgPtNPs from the ethanolic extract of *V. mespilifolia* followed a method previously described (Unuofin et al., 2017). Briefly, the ABTS radical was formed by reacting solutions of 7 mM ABTS and 2.45 mM potassium persulfate for a period of 12 h at room temperature in the dark. A working solution was developed by mixing 1 mL ABTS radical with 60 mL of methanol, and

the absorbance was adjusted to 0.700 ± 0.008 at 734 nm. Thereafter, 100 μL of the ABTS solution was mixed with 100 μL of each extract/standard (25 to 400 $\mu\text{g}/\text{mL}$). The absorbance of the resulting mixture was read at 734 nm after 7 min of incubation in the dark. All samples were run in triplicates. The ABTS radical-scavenging potential of the extracts/standard was determined using the following equation:

$$\text{ABTSScavengingactivity}(\%) = \frac{\text{Abscontrol} - \text{Absample}}{\text{Abscontrol}} \times 100$$

where Abs control is the absorbance of DPPH + methanol and Abs sample is the absorbance of DPPH radical + sample/or standard.

2.9. Ferric reducing antioxidant power (FRAP) assay

The ability of AgNPs and AgPtNPs obtained from the ethanol extract of *Vernonia mespilifolia* to reduce ferric ions was carried out using the method described (Ahmed et al., 2015). The working FRAP reagent used for this study was freshly prepared by mixing 300 mM acetate buffer (pH 3.6), 10 mM TPTZ (tripirydyl triazine) solution, and 20 mM $\text{FeCl}_3 \cdot 6\text{H}_2\text{O}$ solution at a ratio of 10:1:1 respectively. Briefly, 50 μL of each nanomaterial (1 mg/mL) and 50 μL of the standard solutions of gallic acid (20 to 100 $\mu\text{g}/\text{mL}$) was added to 950 μL of FRAP working reagent. Absorbance was read at 593 nm after 15 min of adding the working reagent. The blank sample consisted of 950 μL of FRAP working reagent and 50 μL of methanol. The reducing power capability of the various extracts was expressed as an equivalent concentration of antioxidants that gave a ferric reducing ability equivalent when compared to the gallic acid standard (GAE).

$$\text{GAE} = \frac{CV}{M}$$

where GAE = gallic acid equivalent of sample extract (mg GAE/g of sample);

C = concentration of gallic acid extrapolated from the standard curve in mg/mL;

V = volume of the sample extract in mL;

M = weight of the sample extract in g

2.10. Preparation of the microbial suspension

Microorganisms were standardized using the method of CLSI guidelines (Wiegand et al., 2008). All the tested microbes were grown in nutrient broth for 24 h, followed by the matching of bacterial suspension to the turbidity equivalent to 0.5 McFarland solution (1×10^8 CFU/mL) with the addition of sterile saline.

2.11. Antimicrobial activity

The antimicrobial activity of the synthesized AgPtNPs was tested using the serial dilution method (Elisha et al., 2017) against one gram-positive bacterium (*Staphylococcus aureus*) (ATCC: 25923), a multidrug-resistant gram-negative bacterium (*Escherichia coli*) (ATCC: 25922), and a fungus (*Candida albicans*) (ATCC: 10231) (Anatech, Kwik-stick®). A 1 mg/mL AgPtNPs dispersed in deionized water (stock solution) was prepared and serially diluted in a 96 well plate with

an overnight culture of microorganisms to a final concentration range of 7.8–1000 $\mu\text{g/mL}$. The AgNPs was used as a control for the experiment. Plates were incubated at 37 °C for 24 h, and 20 μL of 0.2 mg/mL of the microbial growth indicator Resazurin dye (Sigma-Aldrich®) was added to all wells. All experiments were performed in triplicate.

2.12. Cytotoxicity assay

The MTT reduction assay was used to assess the cytotoxicity of the nanoparticles on human embryonic kidney (HEK 293) and human breast cancer (MCF-7) cell lines. Cells were grown in tissue culture flasks and harvested using 2% trypsin in DMEM. Cells were counted and 100 μL of cells were seeded into a 96 well plate (5×10^4 cells/well) and the plates incubated for 24 h at 37 °C with 5% CO_2 . After incubation, the media were aspirated and treated with 100 μL of varying concentrations of dispersions of AgPtNPs and AgNPs in culture media and incubated for 24 h. The plates were treated with 20 μL (5 mg/mL) MTT solution and incubated for another 3 h. Afterwards, the media were carefully removed and then DMSO were added to dissolve the formazan crystals. The plates were read at 570 nm using an ELISA plate reader (ThermoFisher Scientific, Varioskan Flash, Finland) and the mean of the triplicate results calculated.

2.13. Data analysis

All assays were conducted in triplicate, and the obtained results were expressed as (mean \pm SD). Statistical analysis was done using MINITAB 17 and a one-way ANOVA by Fischer's least significant difference (LSD) to determine significant differences in all parameters. Values were considered statistically significant at $*p < 0.05$.

3. Results and discussion

3.1. Preparation and characterization

Preliminary phytochemical screening of the EVM plant extract confirmed the presence of bioactive compounds such as polyphenols, proanthocyanidins, tannins, and flavonoids,

thereby confirming its use as an eco-friendly means of synthesizing metal nanoparticles (Unuofin et al., 2018). The bioreduction of mixed Ag and Pt ions to form AgPtNPs using EVM extract was monitored using UV–vis spectroscopy with the reaction completed in 1 h. A final brownish-green color was observed indicating the formation of AgPtNPs (Fig. 1). The UV–vis spectra of the EVM capped AgPtNPs showed surface plasmon resonance (SPR) at 415 nm after 60 min (Fig. 2A). Unlike core–shell bimetallic nanoparticles, which display two bands, the single band formation in the region of Ag likely indicated that more of the Ag than Pt was reduced. Hence, we suspected the possible formation of a nanoalloy (Elemike et al., 2019; Xia et al., 2013). The monometallic AgNPs control showed a characteristic peak appearing at approximately 413 nm (Fig. S1). The peaks at 538, 610, and 672 nm could be ascribed to some intensely absorbed bioorganic oxidation products originating from the extracts (Elemike et al., 2019).

The TEM image of the AgPtNPs synthesized from the dried EVM extract showed predominantly spherical shaped nanoparticles (Fig. 2B) with a mean diameter of 35.5 ± 0.8 nm (Fig. S2) and polydispersity index (PDI) of 0.2. The average particle diameter calculated for AgNPs was 33.4 ± 1.0 nm with a spherical morphology (Fig. S3). Both AgPtNPs and AgNPs were of mean diameter lower than 40 nm, which have been reported to easily taken up by cells and can enter the nucleus (Wu et al., 2019). The energy-dispersive X-ray (EDS) spectra (Fig. 2C) showed peak signals from Ag and Pt, indicating that both metals were present in the extract synthesized nanoparticles. Similarly, the EDS spectra of the control AgNPs contained Ag elemental presence (Fig. S4). The Cu signals were attributed to the carbon coated copper grid upon which the nanoparticle samples were drop-dried for the analysis. The bright spots in the selected area electron diffraction pattern (SAED) showed that the formed AgPtNPs are crystalline (Fig. 2D). The results corresponded with the absorption spectra data and demonstrated the efficiency of the EVM to form metallic nanostructures.

3.1.1. FTIR analysis

The FTIR spectrum of the dried EVM extract (Fig. 3) showed peaks at 3331, 2918, 1736, 1602, 1377, 1263, and a strong and intense peak at 1028 cm^{-1} . The peak at 3331 cm^{-1} represents a strong hydroxyl group found mostly in phenolics, carbohydrates, and flavonoids. The peaks at 2918, 1736,

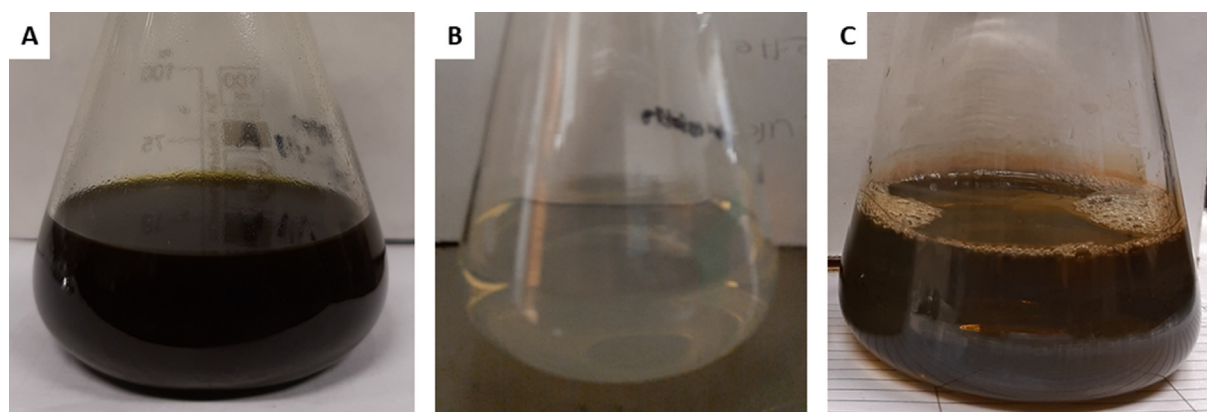


Fig. 1 Photographs showing the color of whole plant ethanolic extract (A), Ag and Pt mixed solution (B), and colloidal AgPtNPs nanoparticles (C).

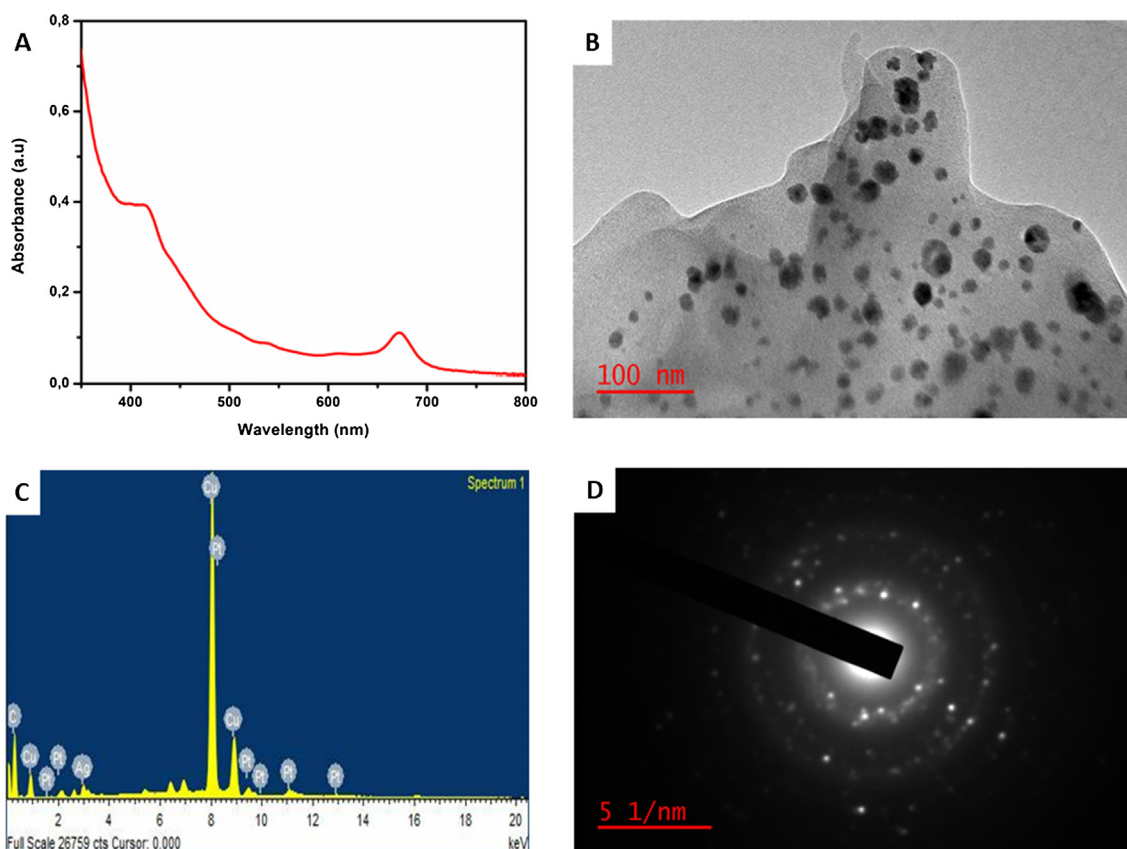


Fig. 2 UV-vis absorption spectra (A), TEM image (B) EDS spectra (C), and SAED (D) of the extract synthesized AuPtNPs.

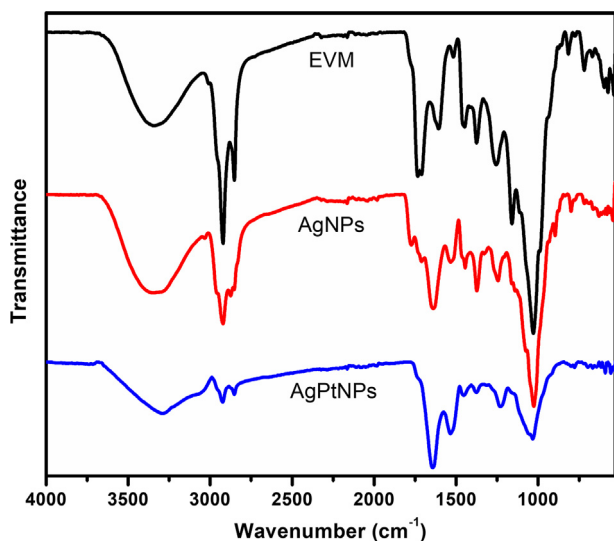


Fig. 3 Fourier transform infrared spectra of dried *V. mespilifolia* (EVM) leaf extract before and after biosynthesis of AgNPs and AgPtNPs.

1602, 1377, 1263, and 1028 cm^{-1} are associated with C-H (stretching), C = O (carboxylic stretching), N-H (bending), O-H (carboxylic bending), C-N (primary aromatic amine stretching), and C-C (stretching) respectively. The presence of almost all these characteristic peaks of EVM in the biosynthesized AgNPs and AgPtNPs strongly indicated effective cap-

ping and stabilization of the nanoparticles. The intensity of the peaks of AgNPs and AgPtNPs was reduced, as shown in their spectra, thus indicating a reduced concentration of EVM extract in the stabilization and possible conjugation with the nanoparticles. These results support the key role that EVM extract played in the reduction of the metal ions to their corresponding metal nanoparticles.

3.1.2. Nanoparticles stability

The stability of the purified nanoparticles dispersed in water was measured for 7 days using a dynamic light scattering (DLS) technique. The AgNPs and AgPtNPs showed a negligible zeta-potential value increase during this period (Fig. 4). The negative charges may be attributed to the strong adsorption of plant phytochemicals on the formed nanoparticles, thereby improving their stability and preventing aggregation (Elemike et al., 2019). Similarly, a polydispersity index (PDI) of 0.2 was calculated for AgPtNPs. A low degree of dispersity indicated the good quality and monodispersity of the AgPtNPs with respect to the particle size distribution which is beneficial for biological activity. The PDI and size distribution are highly essential properties as it affect the stability, cellular uptake, accumulation, and ultimately the biological performance induced by nanoparticles (Danaei et al., 2018).

3.2. Phytochemical constituents

We investigated the role of polyphenolic compounds in the biosynthesis of AgNPs and AgPtNPs from an ethanol extract of *V. mespilifolia* by quantifying the total phenolic content

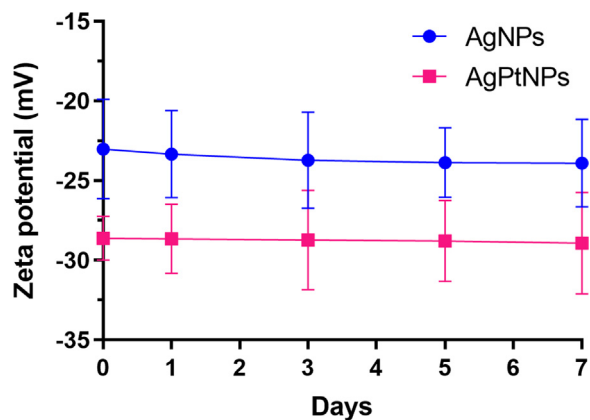


Fig. 4 Zeta-potentials of the extract synthesized AgNPs and AgPtNPs measured for 7 days. Data are presented as mean \pm standard deviation ($n = 3$).

(TPC), total flavonoids content (TFC), and proanthocyanidins (PA) content at baseline (0 min) and after 60 min of reaction time. The information from the above is essential in highlighting the possible mechanism of the reaction. Phenols, flavonoids, proanthocyanins, polyamines, and polyamides belong to a family known as polyphenolic compounds. In recent times, phenols, flavonoids, and proanthocyanins have been shown to possess the ability to donate an electron, act as metal chelators, and as singlet and triplet oxygen quenchers (Bakhtiar et al., 2015; Unuofin et al., 2018). In our previous study, ethanol extract of *V. mespilifolia* showed the presence of 106.9 ± 0.0 mg GAE/g dry weight TPC, 464.7 ± 0.0 mg QE/g dry weight TFC, and 83.9 ± 0.0 mg CE/g dry weight PA (Unuofin et al., 2018). In the synthesized nanoparticles (AgNPs and AgPtNPs), a reduction in the amount of TPC (28.0 ± 0.9 and 13.6 ± 0.1 mg GAE/g dry weight) and TFC (366.2 ± 17.0 and 126.6 ± 0.3 mg QE/g dry weight) was observed, while the PA content of AgNPs increased as shown in Table 1. The reduction observed mainly in the TPC and TFC of AgNPs and AgPtNPs and PA of AgPtNPs after 60 min of synthesis could be attributed to the nucleophilic nature of the aforementioned phytochemicals, which play a

Table 1 Polyphenolic content of AgNPs and AgPtNPs synthesized from the ethanol extract of *Vernonia mespilifolia*.

Samples	TPC (mg GAE/g)	TFC (mg QE/g)	PA (mg CE/g)
AgNPs EVM	28.0 ± 0.9^a	366.2 ± 17.0^a	161.9 ± 0.6^a
AgPtNPs EVM	13.6 ± 0.1^b	126.6 ± 0.3^b	70.2 ± 0.6^b

Abbreviations: Total phenol content (TPC) mg GAE/g, milligram gallic acid equivalent per gram of extract; total flavonoid content (TFC) mg QE/g, milligram quercetin equivalent per gram of extract; Proanthocyanins (PA) mg CE/g, milligram catechin equivalent per gram of extract.

Values are expressed as the mean \pm standard deviation.

All superscripts indicated a significant difference ($P < 0.05$) between the means. Values within the same column with different superscripts are significantly different.

major role in the reduction and chelation of transitional metals and also aid in stabilizing them (Raghunandan et al., 2010; Sivaraman et al., 2009).

3.3. Antioxidant activity

The antioxidant activities of synthesized AgNPs and AgPtNPs were evaluated by DPPH, ABTS, and FRAP assays, with ascorbic acid being used as a standard. The DPPH and ABTS radical scavenging abilities of AgNPs and AgPtNPs are shown in Fig. 5. These biosynthesized nanoparticles exhibited great potential in scavenging free radicals in a dose-dependent manner. The AgPtNPs showed a greater ability to scavenge free radicals, especially DPPH and ABTS (IC_{50} 19.5 and 21.6 μ g/mL) respectively, comparable to AgNPs and ascorbic acid, as shown in Table 1. The AgPtNPs showed a markedly higher inhibition of DPPH radicals compared to ABTS. The FRAP assay estimates the reducing potential of an antioxidant substance reacting with a ferric tripyridyltriazine complex, thus yielding a colored ferrous tripyridyltriazine. In this assay, free radical chains are broken via the donation of a hydrogen atom. FRAP values of AgNPs and AgPtNPs were 18.5 and

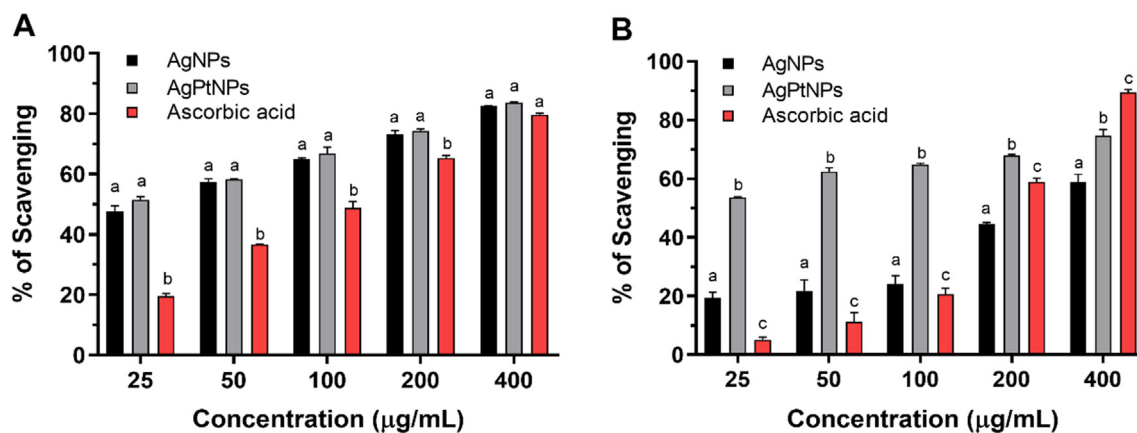


Fig. 5 Inhibition of DPPH radicals (A) and ABTS radicals (B) by AgNPs and AgPtNPs synthesized from the ethanol extract of *Vernonia mespilifolia*.

Table 2 IC₅₀ and FRAP values of AgNPs and AgPtNPs synthesized from the ethanol extract of *Vernonia mespilifolia* and ascorbic acid.

Samples/Standard	ABTS IC ₅₀ (µg/mL)	DPPH IC ₅₀ (µg/mL)	FRAP (mg GAE/g)
AgNPs	302.7 ± 2.8a	28.5 ± 0.1a	18.5 ± 0.2a
AgPtNPs	21.6 ± 2.1b	19.5 ± 0.2b	44.1 ± 2.7b
Ascorbic acid	210.7 ± 1.0c	131.8 ± 0.4c	–

Abbreviations: IC₅₀, concentration (mg/mL) required to scavenge/inhibit 50% of the radical.

Values obtained from regression lines with a 95% confidence level.

44.1 mg GAE/g of the nanomaterials respectively, as shown in Table 2.

In the present study, the bimetallic AgPtNPs system was found to possess superior antioxidant activity compared with AgNPs and ascorbic acid as determined by DPPH, ABTS, and FRAP radical scavenging methods, as shown in Table 2. The antioxidant activity exhibited by nanoparticles may be due to the phytochemicals present in the ethanol extract of *V. mespilifolia*, already known for their antioxidant potential (Unuofin et al., 2018), which form the part of synthesized nanoparticles as capping agents (Meena Kumari et al., 2015; Reddy et al., 2014; Xia et al., 2013).

3.4. Antimicrobial activity

The antimicrobial activity of the synthesized AgPtNPs was evaluated against *Staphylococcus aureus*, *Escherichia coli*, and *Candida albicans* at a concentration range of 7.8–1000 µg/mL. For control, AgNPs was used under similar conditions in the

Table 3 Minimum inhibitory concentration (MIC = µg/mL) of extract-reduced AgNPs and AgPtNPs.

Nanoparticles (NPs)	<i>S. aureus</i>	<i>E. coli</i>	<i>C. albicans</i>
AgNPs	62.5	500.0	250.0
AgPtNPs	32.5	250.0	125.0

experiment. As shown in Table 3, the synthesized AgPtNPs showed significant antimicrobial activity against the tested pathogens. The minimum inhibitory concentration (MIC) of AgPtNPs had the strongest inhibitory activity against the gram-positive strain (*S. aureus*) with an MIC of 32.5 µg/mL, followed by 250 and 125 µg/mL against *E. coli* and *C. albicans*, respectively. These MIC values represented a two-fold inhibitory activity demonstrated by the AgPtNPs on the pathogens compared to AgNPs. On the other hand, a lower inhibition was observed in the multi-drug resistant bacteria, *E. coli*. A recent study by Ruiz et al., investigated the antimicrobial effect of chemically synthesized AgPtNPs and observed enhanced inhibitory activity against medically important pathogens (Ruiz et al., 2020).

3.5. Cytotoxic activity

The possible cytotoxic effects of the extract-synthesized AgNPs and AgPtNPs against normal human embryonic kidney cells (HEK 293) and human breast cancer cells (MCF-7) were performed. As shown in Fig. 6A, HEK 293 cells responded to the cytotoxic effects of AgNPs and AgPtNPs in a dose-dependent manner. Both AgNPs and AgPtNPs were relatively non-toxic to normal cells (HEK 293) with more than 60% cell viability at a concentration of 12.5 µg/mL. A lethal dose (LD₅₀) value of 54.5 µg/mL and 60.0 µg/mL were calculated for AgNPs and AgPtNPs respectively. A similar dose-response effect was noticed for AgNPs and AgPtNPs in MCF-7 cells. However, AgPtNPs exhibited significant cytotoxic activity compared to AgNPs (Fig. 6B). For example, AgPtNPs demonstrated a remarkable ability to inhibit the proliferation of cancer cells at a concentration of 6.25–100 µg/mL. As shown in Table 4, an LD₅₀ of 10.2 µg/mL was calculated for AgPtNPs, while AgNPs showed an LD₅₀ value of 27.1 µg/mL. The results obtained revealed the variability in LD₅₀ values with the AgPtNPs showing a higher cytotoxic effect in cancerous cells compared to normal cells. We could attribute the enhanced cytotoxicity to the synergistic effect of Ag and Pt as reported (Ghosh et al., 2015).

Our results suggested a selective cytotoxic mechanism of action, which may be attributed to several factors. These

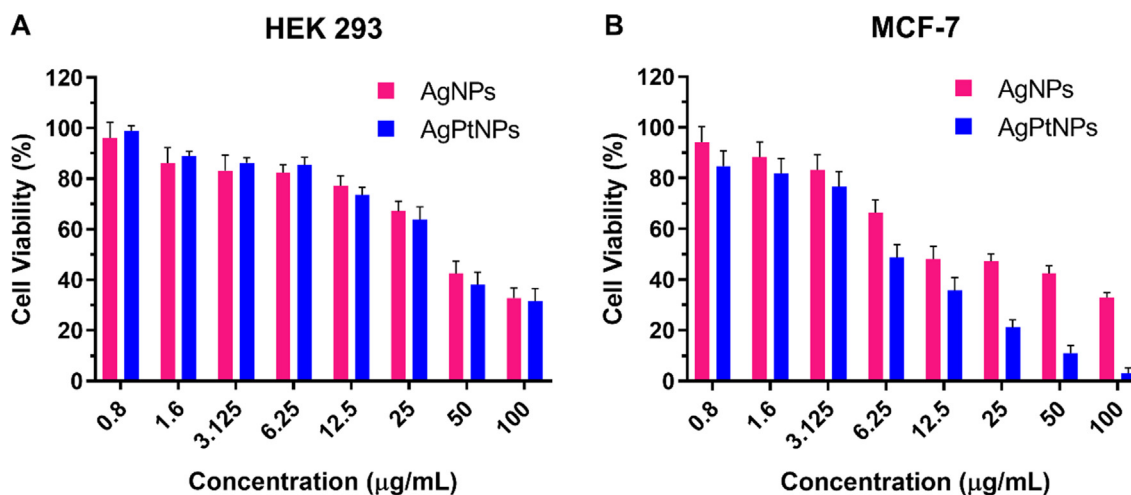


Fig. 6 Cell viability assay of AgNPs and AgPtNPs against (A) HEK 293 and (B) MCF-7 cells. Data are expressed as a percentage of the control (always 100%) and are represented as mean ± standard deviation (SD).

Table 4 Lethal concentrations (LC₅₀ = µg/mL) of extract-reduced AgNPs and AgPtNPs on HEK 293 and MCF-7 cells.

Nanoparticles (NPs)	HEK 293 (LC ₅₀)	MCF-7 (LC ₅₀)
AgNPs	54.5	27.1
AgPtNPs	60.0	10.2

factors include the physicochemical properties of the nanoparticles, possible tightly packed alloyed systems in which the diffusion of either Ag or Pt ions was restricted, induction of cellular DNA damage, metabolic expressions in the cells, and synergistic effects of the extract and the nanoparticles.

4. Conclusions

This study highlights the potential of *V. mespilifolia* extract in synthesizing bimetallic AgPt alloyed nanoparticles. The particles were monodispersed with a size of 35.5 ± 0.8 nm, and a negative zeta potential value (-28.6 mV) demonstrated their stability. The AgPtNPs showed a greater ability to scavenge free radicals, especially DPPH and ABTS, when compared with AgNPs and ascorbic acid. The enhanced antioxidant properties of AgPtNPs can inhibit cancer proliferation as well as induce apoptotic cell death. Besides, the AgPtNPs exhibited potential antimicrobial activity and cytotoxicity in a dose-responsive manner, with selective cytotoxicity towards cancer cells compared to normal cells, thereby necessitating the rationale to designing and harnessing these synergistic effects for biomedical applications.

Acknowledgments

The authors would like to thank the Nanotechnology and Water Sustainability Research Unit (NanoWS) and the College of Agriculture and Environmental Sciences (CAES) through the University of South Africa (UNISA) for support.

Declaration of Competing Interest

All authors declare no competing interests.

Appendix A. Supplementary material

Supplementary data to this article can be found online at <https://doi.org/10.1016/j.arabjc.2020.06.019>.

References

- Adebayo, A.E., Oke, A.M., Lateef, A., Oyatokun, A.A., Abisoye, O. D., Adiji, I.P., Fagbenro, D.O., Amusan, T.V., Badmus, J.A., Asafa, T.B., Beukes, L.S., Gueguim-Kana, E.B., Abbas, S.H., 2019. Biosynthesis of silver, gold and silver-gold alloy nanoparticles using *Persea americana* fruit peel aqueous extract for their biomedical properties. *Nanotechnol. Environ. Eng.* 4, 1–15. <https://doi.org/10.1007/s41204-019-0060-8>.
- Afolayan, A.J., Mbaebie, B.O., 2010. Ethnobotanical study of medicinal plants used as anti-obesity remedies in Nkonkobe Municipality of South Africa. *Pharmacogn. J.* 2, 368–373. [https://doi.org/10.1016/S0975-3575\(10\)80017-3](https://doi.org/10.1016/S0975-3575(10)80017-3).
- Ahmed, D., Khan, M., Saeed, R., 2015. Comparative analysis of phenolics, flavonoids, and antioxidant and antibacterial potential of methanolic, hexanic and aqueous extracts from *Adiantum caudatum* leaves. *Antioxidants* 4, 394–409. <https://doi.org/10.3390/antiox4020394>.
- Bakhtiar, S.I., Shahriar, M., Akhter, R., Bhuiyan, M.A., 2015. In vitro antioxidant activities of the whole plant extract of *Chrozophora prostrata* (dalz.). *Ann. Biol. Res.* 6, 19–26.
- Baskaran, B., Muthukumarasamy, A., Chidambaram, S., Sugumaran, A., Ramachandran, K., Manimuthu, T.R., 2017. Cytotoxic potentials of biologically fabricated platinum nanoparticles from *Streptomyces* sp. on MCF-7 breast cancer cells. *IET Nanobiotechnol* 11, 241–246. <https://doi.org/10.1049/iet-nbt.2016.0040>.
- Breisch, M., Grasmik, V., Loza, K., Pappert, K., Rostek, A., Ziegler, N., Ludwig, A., Heggen, M., Epple, M., Tiller, J.C., Schildhauer, T.A., Köller, M., Sengstock, C., 2019. Bimetallic silver-platinum nanoparticles with combined osteo-promotive and antimicrobial activity. *Nanotechnology* 30, 1–10. <https://doi.org/10.1088/1361-6528/ab172b>.
- Danaei, M., Dehghankhold, M., Ataei, S., Hasanzadeh Davarani, F., Javanmard, R., Dokhani, A., Khorasani, S., Mozafari, M.R., 2018. Impact of particle size and polydispersity index on the clinical applications of lipidic nanocarrier systems. *Pharmaceutics* 10, 1–17. <https://doi.org/10.3390/pharmaceutics10020057>.
- Ding, Y., Fan, F., Tian, Z., Wang, Z.L., 2010. Atomic structure of Au-Pd bimetallic alloyed nanoparticles. *J. Am. Chem. Soc.* 132, 12480–12486. <https://doi.org/10.1021/ja105614q>.
- Dold, A.P., Cocks, M.L., 2001. Traditional veterinary medicine in the Alice district of the Eastern Cape Province, South Africa. *S. Afr. J. Sci.* 97, 375–379.
- Elegbede, J.A., Lateef, A., Azeed, M.A., Asafa, T.B., Yekeen, T.A., Oladipo, I.C., Hakeem, A.S., Beukes, L.S., Gueguim-Kana, E.B., 2019. Silver-gold alloy nanoparticles biofabricated by fungal xylanases exhibited potent biomedical and catalytic activities. *Biotechnol. Prog.* 35, 1–13. <https://doi.org/10.1002/btpr.2829>.
- Elemike, E.E., Onwudiwe, D.C., Nundkumar, N., Singh, M., Iyekowa, O., 2019. Green synthesis of Ag, Au and Ag-Au bimetallic nanoparticles using *Stigmaphyllon ovatum* leaf extract and their in vitro anticancer potential. *Mater. Lett.* 243, 148–152. <https://doi.org/10.1016/j.matlet.2019.02.049>.
- Elisha, I.L., Botha, F.S., McGaw, L.J., Eloff, J.N., 2017. The antibacterial activity of extracts of nine plant species with good activity against *Escherichia coli* against five other bacteria and cytotoxicity of extracts. *BMC Complement. Altern. Med.* 17, 133. <https://doi.org/10.1186/s12906-017-1645-z>.
- Fakayode, O.J., Oladipo, A.O., Oluwafemi, O.S., Songca, S.P., 2016. Biopolymer-mediated green synthesis of noble metal nanostructures. *Recent Adv. Biopolym.* 19–42. <https://doi.org/10.5772/62127>.
- Ghosh, S., Nitnavare, R., Dewle, A., Tomar, G.B., Chippalkatti, R., More, P., Kitture, R., Kale, S., Bellare, J., Chopade, B.A., 2015. Novel platinum-palladium bimetallic nanoparticles synthesized by *Dioscorea bulbifera*: anticancer and antioxidant activities. *Int. J. Nanomed.* 10, 7477–7490. <https://doi.org/10.2147/IJN.S91579>.
- Grasmik, V., Breisch, M., Loza, K., Heggen, M., Köller, M., Sengstock, C., Epple, M., 2018. Synthesis and biological characterization of alloyed silver-platinum nanoparticles: from compact core-shell nanoparticles to hollow nanoalloys. *RSC Adv.* 8, 38582–38590. <https://doi.org/10.1039/c8ra06461j>.
- Hanen, F., Riadh, K., Samia, O., Sylvain, G., Christian, M., Chedly, A., 2009. Interspecific variability of antioxidant activities and phenolic composition in *Mesembryanthemum* genus. *Food Chem. Toxicol.* 47, 2308–2313. <https://doi.org/10.1016/j.fct.2009.06.025>.
- John Leo, A., Oluwafemi, O.S., 2017. Plant-mediated synthesis of platinum nanoparticles using water hyacinth as an efficient biomatrix source – an eco-friendly development. *Mater. Lett.* 196, 141–144. <https://doi.org/10.1016/j.matlet.2017.03.047>.

- Khan, R.A., Khan, M.R., Sahreen, S., Ahmed, M., 2012. Evaluation of phenolic contents and antioxidant activity of various solvent extracts of *Sonchus asper* (L.). *Hill. Chem. Cent. J.* 6, 12. <https://doi.org/10.1186/1752-153X-6-12>.
- Manikandan, M., Hasan, N., Wu, H.F., 2013. Platinum nanoparticles for the photothermal treatment of Neuro 2A cancer cells. *Biomaterials* 34, 5833–5842. <https://doi.org/10.1016/j.biomaterials.2013.03.077>.
- McGaw, L.J., Lall, N., Meyer, J.J.M., Eloff, J.N., 2008. The potential of South African plants against *Mycobacterium* infections. *J. Ethnopharmacol.* 119, 482–500. <https://doi.org/10.1016/j.jep.2008.08.022>.
- Meena Kumari, M., Jacob, J., Philip, D., 2015. Green synthesis and applications of Au-Ag bimetallic nanoparticles. *Spectrochim. Acta - Part A Mol. Biomol. Spectrosc.* 137, 185–192. <https://doi.org/10.1016/j.saa.2014.08.079>.
- Mohan, S., Oluwafemi, O.S., George, S.C., Jayachandran, V.P., Lewu, F.B., Songca, S.P., Kalarikkal, N., Thomas, S., 2014. Completely green synthesis of dextrose reduced silver nanoparticles, its antimicrobial and sensing properties. *Carbohydr. Polym.* 106, 469–474. <https://doi.org/10.1016/j.carbpol.2014.01.008>.
- Mokoka, T.A., Xolani, P.K., Zimmermann, S., Hata, Y., Adams, M., Kaiser, M., Moodley, N., Maharaj, V., Koorbanally, N.A., Hamburger, M., Brun, R., Fouche, G., 2013. Antiprotozoal screening of 60 South African plants, and the identification of the antitrypanosomal germacranolides schkuhrin I and II. *Planta Med.* 79, 1380–1384. <https://doi.org/10.1055/s-0033-1350691>.
- Nath, D., Banerjee, P., 2013. Green nanotechnology – a new hope for medical biology. *Environ. Toxicol. Pharmacol.* 36, 997–1014. <https://doi.org/10.1016/j.etap.2013.09.002>.
- Ojha, A.K., Forster, S., Kumar, S., Vats, S., Negi, S., Fischer, I., 2013. Synthesis of well-dispersed silver nanorods of different aspect ratios and their antimicrobial properties against gram positive and negative bacterial strains. *J. Nanobiotechnol.* 11, 42. <https://doi.org/10.1186/1477-3155-11-42>.
- Oladipo, A.O., Iku, S.I.I., Ntwasa, M., Nkambule, T.T.I., Mamba, B. B., Msagati, T.A.M., 2020a. Doxorubicin conjugated hydrophilic AuPt bimetallic nanoparticles fabricated from *Phragmites australis*: Characterization and cytotoxic activity against human cancer cells. *J. Drug Deliv. Sci. Technol.* 57, . <https://doi.org/10.1016/j.jddst.2020.101749> 101749.
- Oladipo, A.O., Nkambule, T.T.I., Mamba, B.B., Msagati, T.A.M., 2020b. The stimuli-responsive properties of doxorubicin adsorbed onto bimetallic Au@Pd nanodendrites and its potential application as drug delivery platform. *Mater. Sci. Eng. C* 110. <https://doi.org/10.1016/j.msec.2020.110696>.
- Oladipo, A.O., Oluwafemi, O.S., Songca, S.P., Sukhbaatar, A., Mori, S., Okajima, J., Komiya, A., Maruyama, S., Kodama, T., 2017. A novel treatment for metastatic lymph nodes using lymphatic delivery and photothermal therapy. *Sci. Rep.* 7, 45459. <https://doi.org/10.1038/srep45459>.
- Olajire, A.A., Kareem, A., Olaleke, A., 2017. Green synthesis of bimetallic Pt@Cu nanostructures for catalytic oxidative desulfurization of model oil. *J. Nanostructure Chem.* 7, 159–170. <https://doi.org/10.1007/s40097-017-0223-8>.
- Pan, Y.T., Yan, Y., Shao, Y.T., Zuo, J.M., Yang, H., 2016. Ag-Pt compositional intermetallics made from alloy nanoparticles. *Nano Lett.* 16, 6599–6603. <https://doi.org/10.1021/acs.nanolett.6b03302>.
- Raghunandan, D., Bedre, M.D., Basavaraja, S., Sawle, B., Manjunath, S.Y., Venkataraman, A., 2010. Rapid biosynthesis of irregular shaped gold nanoparticles from macerated aqueous extracellular dried clove buds (*Syzygium aromaticum*) solution. *Colloids Surfaces B Biointerfaces* 79, 235–240. <https://doi.org/10.1016/j.colsurfb.2010.04.003>.
- Reddy, N.J., Nagoor Vali, D., Rani, M., Rani, S.S., 2014. Evaluation of antioxidant, antibacterial and cytotoxic effects of green synthesized silver nanoparticles by *Piper longum* fruit. *Mater. Sci. Eng. C* 34, 115–122. <https://doi.org/10.1016/j.msec.2013.08.039>.
- Robinson, H., Funk, V.A., 2014. *Gymnanthemum koekemoerae* (Compositae, Vernoniaeae), a new species from South Africa. *PhytoKeys* 2014, 59–65. <https://doi.org/10.3897/phytokeys.36.7386>.
- Ruiz, A.L., Garcia, C.B., Gallón, S.N., Webster, T.J., 2020. Novel silver-platinum nanoparticles for anticancer and antimicrobial applications. *Int. J. Nanomedicine* 15, 169–179. <https://doi.org/10.2147/IJN.S176737>.
- Seethapathy, V., Sudarsan, P., Pandey, A.K., Pandiyan, A., Kumar, T. H.V., Sanjeevi, K., Sundramoorthy, A.K., Krishna Moorthy, S.B., 2019. Synergistic effect of bimetallic Cu: Ni nanoparticles for the efficient catalytic conversion of 4-nitrophenol. *New J. Chem.* 43, 3180–3187. <https://doi.org/10.1039/c8nj05649h>.
- Sharma, G., Kumar, A., Sharma, S., Naushad, M., Prakash Dwivedi, R., AlOthman, Z.A., Mola, G.T., 2019. Novel development of nanoparticles to bimetallic nanoparticles and their composites: a review. *J. King Saud Univ. - Sci.* 31, 257–269. <https://doi.org/10.1016/j.jksus.2017.06.012>.
- Sivaraman, S.K., Elango, I., Kumar, S., Santhanam, V., 2009. A green protocol for room temperature synthesis of silver nanoparticles in seconds. *Curr. Sci.* 97, 1055–1059.
- Srinoi, P., Chen, Y.-T., Vittur, V., Marquez, M., Lee, T., 2018. Bimetallic nanoparticles: enhanced magnetic and optical properties for emerging biological applications. *Appl. Sci.* 8, 1106. <https://doi.org/10.3390/app8071106>.
- Unuofin, J.O., Otunola, G.A., Afolayan, A.J., 2019. Inhibition of key enzymes linked to obesity and cytotoxic activities of whole plant extracts of *Vernonia mespilifolia* less. *Processes* 7. <https://doi.org/10.3390/pr7110841>.
- Unuofin, J.O., Otunola, G.A., Afolayan, A.J., 2018. Polyphenolic content, antioxidant and antimicrobial activities of *vernonia mespilifolia* less. Used in folk medicine in the Eastern Cape Province, South Africa. *J. Evidence-Based Integr. Med.* 23, 1–9. <https://doi.org/10.1177/2515690X18773990>.
- Unuofin, J.O., Otunola, G.A., Afolayan, A.J., 2017. Phytochemical screening and in vitro evaluation of antioxidant and antimicrobial activities of *Kedrostis africana* (L.) Cogn. *Asian Pac. J. Trop. Biomed.* 7, 901–908. <https://doi.org/10.1016/j.apjtb.2017.09.008>.
- Wiegand, I., Hilpert, K., Hancock, R.E.W., 2008. Agar and broth dilution methods to determine the minimal inhibitory concentration (MIC) of antimicrobial substances. *Nat. Protoc.* 3, 163–175. <https://doi.org/10.1038/nprot.2007.521>.
- Wu, M., Guo, H., Liu, L., Liu, Y., Xie, L., 2019. Size-dependent cellular uptake and localization profiles of silver nanoparticles. *Int. J. Nanomedicine* 14, 4247–4259. <https://doi.org/10.2147/IJN.S201107>.
- Xia, B., He, F., Li, L., 2013. Preparation of bimetallic nanoparticles using a facile green synthesis method and their application. *Langmuir* 29, 4901–4907. <https://doi.org/10.1021/la400355u>.
- Zhang, M., Zhao, Y., Yan, L., Peltier, R., Hui, W., Yao, X., Cui, Y., Chen, X., Sun, H., Wang, Z., 2016. Interfacial engineering of bimetallic Ag/Pt nanoparticles on reduced graphene oxide matrix for enhanced antimicrobial activity. *ACS Appl. Mater. Interfaces* 8, 8834–8840. <https://doi.org/10.1021/acsami.6b01396>.
- Zhang, N., Chen, F., Wu, X., Wang, Q., Qaseem, A., Xia, Z., 2017. The activity origin of core-shell and alloy AgCu bimetallic nanoparticles for the oxygen reduction reaction. *J. Mater. Chem. A* 5, 7043–7054. <https://doi.org/10.1039/C6TA10948A>.